Eur. Phys. J. A **6**, 289–302 (1999)

THE EUROPEAN PHYSICAL JOURNAL A

Gamma-ray spectroscopy of $^{192-195}$Po

K. Helariutta[1], J.F.C. Cocks[1], T. Enqvist[1,a], P.T. Greenlees[1], P. Jones[1], R. Julin[1], S. Juutinen[1], P. Jämsen[1], H. Kankaanpää[1], H. Kettunen[1], P. Kuusiniemi[1], M. Leino[1], M. Muikku[1], M. Piiparinen[1], P. Rahkila[1], A. Savelius[1], W.H. Trzaska[1], S. Törmänen[1,b], J. Uusitalo[1], R.G. Allatt[2], P.A. Butler[2], R.D. Page[2], M. Kapusta[3]

[1] Accelerator Laboratory, Department of Physics, University of Jyväskylä, 40351 Jyväskylä, Finland
[2] Department of Physics, Oliver Lodge Laboratory, University of Liverpool, Liverpool L69 7ZE, UK
[3] Department of Nuclear Electronics, Soltan Institute for Nuclear Studies, 05-400 Otwock-Swierk, Poland

Received: 5 July 1999 / Revised version: 7 September 1999
Communicated by J. Äystö

Abstract. Prompt and delayed γ-rays have been observed from very neutron deficient $^{192-195}$Po nuclei by using the recoil-decay tagging (RDT) and recoil gating techniques. The yrast levels up to the (10^+) state in the ^{192}Po were identified for the first time. Comprehensive data for ^{194}Po rendered it possible to extend the yrast line and to observe several positive and negative parity non-yrast states. In the odd-mass isotopes ^{193}Po and ^{195}Po, favoured and unfavoured states on top of the $13/2^+$ state have been identified. The results are discussed within the simple vibrator and rotor pictures as well as in the framework of coexisting spherical and deformed-intruder structures.

PACS. 27.80.+w $190 \leq A \leq 219$ – 23.20.Lv Gamma transitions and level energies – 21.60.Ev Collective models – 25.70.-z Low and intermediate energy heavy-ion reactions

1 Introduction

Even though the Pb nuclei have a closed proton shell of Z = 82 and should thus exhibit spherical shapes, coexisting deformed states at low excitation energies have been observed in light Pb isotopes [1]. A similar shape coexistence phenomenon is also seen in Hg and Pt nuclei having Z < 82. In all these elements the deformed states minimize their energy near the neutron midshell at N = 104. In Pb, Hg and Pt nuclei the origin of these deformed intruder states is supposed to be the interaction of the open neutron shell with proton particle-hole excitations across the Z = 82 shell gap.

Due to experimental difficulties, information on the very neutron-deficient nuclei with Z > 82 is still scarce and thus the existence of shape coexistence in these nuclei has not been verified. In this respect the Po nuclei with two protons outside the Z = 82 shell form an interesting series of isotopes. In Nilsson-Strutinsky calculations May et al. [2] have predicted a coexisting oblate deformed minimum to come down in energy in light Po isotopes and reach the ground state in ^{192}Po.

The excited levels in the neutron-deficient Po nuclei down to N=108 have previously been studied using both in- and off-beam γ-ray detection and α-decay methods [3–9]. An abrupt drop of the level energies is observed in Po isotopes with N $\leq$ 114. Alber et al. [5] associated it with deformed proton *4p-2h* configurations intruding down in excitation energy. The α-and β-decay studies by the Leuven group [6,9–12] strongly support this view and the picture that the observed level structure results from mixing of the normal and intruder states at low spins.

However, the Rutgers group has presented an alternative explanation, based on observed quadrupole vibrational features of ^{198}Po and ^{196}Po [13]. Their view is that instead of the *4p-2h* proton configurations, the neutron orbitals, especially $i_{13/2}$, are responsible for the sudden energy changes. The further depression of the level energies in ^{192}Po and ^{194}Po is taken as a sign of an evolution towards a more collective, anharmonic vibrator [7, 14]. Younes et al. [15] have also succeeded to reproduce the level structure of the neutron-deficient Po nuclei quite well in the particle-core model (PCM) calculations based on the assumption of two protons outside the Z = 82 shell closure coupled to a vibrating core. However, the behaviour of the low-lying, excited 0^+ states could not be explained with this model.

Recently, Oros et al. [16] have used several theoretical approaches to model the behavior of neutron-deficient Po nuclei. Their calculations support the view of mixing of two coexisting structures to be responsible for the observed perturbation of the energy levels in light Po nuclei. On the other hand, they conclude that the PCM model

[a] Present address: Oliver Lodge Laboratory, University of Liverpool, Liverpool L69 7ZE, UK
[b] Present address: NBI, University of Copenhagen, 2100 Copenhagen, Denmark

Table 1. Details of the experiments

Exp.#	Beam	E_{beam}	I_{beam} [a]	Target (enrichment)	Nuclei studied [b]	γ detection mode	γ detector setup
1	^{36}Ar	178 MeV	20 pnA	^{160}Dy (70%)	^{192}**Po**, ^{193,195}Po	In-beam	DORIS
2	^{28}Si	143 MeV	25 pnA	^{170}Yb (72%)	^{194}**Po**, ^{195}Po	In-beam	DORIS
3	^{28}Si	155 MeV	25 pnA	^{171}Yb (90.4%)	^{194}**Po**, ^{195}Po	In-beam	DORIS
4	^{28}Si	155 MeV	20 pnA	^{171}Yb (90.4%)	^{194}**Po**, ^{195}Po	In-beam, off-beam	Jurosphere, 25% Ge
5	^{36}Ar	196 MeV [c]	38 pnA [c]	^{160}Dy (70%)	(^{191}**Po**,) ^{192}Po	Delayed	25% Ge
6	^{32}S	172 MeV	30 pnA	^{166}Er (>96%)	(^{193}**Po**,) ^{194}Po	Delayed	4 × 25% Ge

[a] Beam intensities (given in units of particles nA) are approximate average values
[b] The nucleus of main interest in the run is marked with bold letters. Nuclei shown in parentheses are not discussed in this work
[c] The beam energy and intensity had several values during the experiment. The maximum energy and intensity were 196 MeV and 38 pnA, respectively

can predict quite well the experimentally observed level properties of Po isotopes with A = 200 - 210. However, it is not able to reproduce the changes occurring in the N < 116 Po isotopes with physically meaningful parameters.

In our earlier work excited states up to $I^{\pi} = (8^{+})$ in ^{192}Po [8] were observed for the first time revealing signs of flattening of the level-energy systematics when going towards the neutron midshell. A similar behavior of level energies has been observed in even-mass Pt nuclei where it has been interpreted as an evidence for a ground state intruder configuration [1]. Based on this observation and the mixing calculations performed by Bijnens et al. [12] the observed excited states of ^{192}Po were assigned to a deformed intruder ground-state band. The measurement for the excited states of ^{192}Po was repeated by Fotiades et al. [14].

Study of odd-mass Po nuclei provides an alternative tool for the examination of shapes of Po isotopes. Fotiades et al. [17] have studied the odd-mass $^{193-197}$Po nuclei and come to the conclusion that in these nuclei the odd $i_{13/2}$ neutron is weakly coupled to a vibrating core. This neutron increases collectivity which is mainly anharmonic vibrational in character.

In order to shed light on the ambiguities discussed above we have performed γ-ray spectroscopic studies of light odd- and even-mass Po nuclei with N = 108 - 111. Due to strong fission competition, the fusion-evaporation reaction channels for populating these Po nuclei become very weak. Therefore, special triggering methods are needed to resolve the events of interest from the vast background. In the present work the $^{192-195}$Po nuclei are studied utilizing the recoil-decay tagging (RDT) [18,19] and recoil gating methods for both prompt and delayed γ rays. The level schemes are extended from the previous ones [7,8,17] giving a possibility for new evaluations on the structure of light Po nuclei.

2 Experimental details

The polonium nuclei studied in this work were produced in several experimental runs. The in-beam γ-ray data were acquired in four experiments. These experiments resulted in new information on excited states of $^{192-195}$Po. Excited states in ^{192}Po were identified for the first time. Results of the preliminary analysis were published earlier in a short report [8]. Some of the data on the isomeric states have been obtained as a side product from the experiments focussed on the α-decay studies of the neutron-deficient odd-mass polonium nuclei ^{191}Po and ^{193}Po [20,21]. In these runs the γ-ray detection system was behind the focal plane particle detector and no prompt γ-ray data were recorded. Details of all the experiments are collected in Table 1.

The experiments were carried out in the accelerator laboratory of the University of Jyväskylä (JYFL) and the beams were provided by the JYFL cyclotron. In all the runs the gas-filled recoil separator RITU [22] was utilized in connection with γ-ray detection systems installed around the target area and/or at the focal plane. The target thicknesses were about 500 $\mu g/cm^2$ in all of the runs to enable the fusion-evaporation residues to fly from the target to the separator and to optimize the yield with respect to their angular spread. In the prompt γ-ray detection, two different Compton-suppressed Ge detector systems were used. The DORIS array consisted of nine TESSA type [23] detectors in a dodecahedron geometry (detectors at angles 78°, 102° and 143° with respect to the beam direction) and had an efficiency of about 0.6% at 1.3 MeV. The Jurosphere array contained 10 TESSA type detectors at angles 79° and 101° and 13 Eurogam phase I type detectors [24] at angles 134° and 158° with respect to the beam direction and had an efficiency of about 1.5% at 1.3 MeV. Thin copper (0.5 mm or 1 mm) or tin (0.25 mm) absorbers were set in front of the Ge detectors to reduce the counting rate due to target X-rays. The maximum counting rates in the Ge detectors around the target position were about 10 kHz.

The fusion-evaporation residues were separated from the dominant fission background by the RITU gas-filled recoil separator. RITU is a charge and velocity focusing device, especially designed for collecting recoiling fusion-evaporation residues with high efficiency. The recoils were implanted on a 80mm × 35mm Si detector horizontally divided into either 8 or 16 vertically position sensitive

strips. The energy resolution of the strip detector for α particles energies was 37 keV in experiments 1-3 and 25 keV in experiments 4-6. The Si detector covers about 70% of the recoil distribution at the focal plane. The transmission for the recoils studied in this work was about 25% and about 50% of the α particles emitted by them are detected. The position sensitivity of the Si detector enables the recoils to be correlated with their subsequent α particles and thus the use of the RDT method where the γ rays emitted by these recoils are identified by using their characteristic α decay. The correlation times used in the RDT analysis ranged from 3 to 5 half-lifes of the nucleus of interest. An example of singles α spectrum from experiment 1 is shown in Fig. 1a). Figure 1b) presents the energies of the α particles observed in the same position as the earlier recoil implantation within the maximum time interval of 170 ms (~ 5 ^{192}Po half-lives). Figures 1a) and b) show how the correlation techniques result in suppression of the background and the peaks from the long-lived α emitters.

In addition to the prompt γ-ray detection around the target position, information on the isomeric states of the Po nuclei was collected with the Ge detectors installed behind the RITU focal plane Si detector. Two focal plane Ge-detector setups were utilized: either a single 25% Ge, positioned at 2 cm distance from the Si detector, or an array of four 25% Ge detectors at about 6 cm from the Si detector. For enabling a close geometry the Ge detectors at the focal plane were not Compton suppressed.

Signals from the Si strip detector for the energy, position and the detection time of the recoils and α particles were recorded, as well as the γ-ray energies and detection times from the Ge detectors at the target position and the focal plane. The data were collected on the tape if an event in the Si detector or a $\gamma\gamma$ event at the target position was observed.

3 Results

3.1 ^{192}Po

Prompt γ rays from ^{192}Po were collected in experiment 1 (see Table 1). The results from the preliminary analysis of the data have been published earlier in the short report [8]. During this experiment, a total of about 35000 ^{192}Po α decays were detected in 120 hours. A half-life of 32.2(3) ms for the ^{192}Po α decay was extracted, being consistent with the value 33.2(14) ms given in literature [12]. An RDT analysis was performed resulting in the prompt ^{192}Po γ-ray spectrum shown in Fig. 2. The energies and intensities of the observed γ-ray transitions are listed in Table 2. Also an α tagged matrix of $\gamma\gamma$ coincidences was created. Even though the number of events in this matrix was small, coincidences between the three lowest transitions could be seen revealing their cascade character. The level scheme shown as an inset in Fig. 2 was constructed supposing that the 262, 343, 438, 518 and 579 keV transitions form an E2 cascade. Ordering of the transitions was based on their observed intensities and Po energy level systematics. Due to the lack of statistics the spin assignments are based on the energy level systematics. According to our assignments levels up to 10^+ are seen. A set of weaker γ rays at energies 406, 431 and 475 keV can also be assigned to ^{192}Po but cannot be placed into the level scheme.

Table 2. γ-ray transitions and energy levels in ^{192}Po

E_γ (keV)	Intensity (%)	E_i (keV)	I_i^π	I_f^π
262.0(3)	100(6)	262	(2^+)	0^+
343.2(3)	89(8)	605	(4^+)	(2^+)
438.1(5)	32(5)	1043	(6^+)	(4^+)
517.9(5)	17(5)	1561	(8^+)	(6^+)
579.4(5)	6(2)	2141	(10^+)	(8^+)
406(1)	9(3)			
431(1)	8(2)			
475(1)	6(2)			

Experiment 5 focussed on the study of the α decay of ^{191}Po [21]. However, about 8500 α particles belonging to the ^{192}Po decay were observed. An RDT method for the focal-plane Ge detector was utilized to search for possible delayed γ-rays from ^{192}Po. The $2^+ \rightarrow 0^+$, $4^+ \rightarrow 2^+$ and $8^+ \rightarrow 6^+$ γ-ray transitions of ^{192}Po were clearly seen in the resulting spectrum. The $6^+ \rightarrow 4^+$ transition was missing, probably due to the insufficient statistics. The observation of these transitions is an indication of the existence of an isomeric state above the 8^+ state having a half-life of the order of one microsecond. No quantitative analysis on the energy or the half-life of the isomer was possible.

3.2 ^{193}Po

In-beam γ-ray data for ^{193}Po were collected as a side product in experiment 1. The nucleus ^{193}Po has two α-decay branches, one from the $3/2^-$ state ($E_\alpha = 6.949$ MeV, $t_{1/2} = 0.45$ s) and the other from the $13/2^+$ state ($E_\alpha = 7.004$ MeV, $t_{1/2} = 0.24$ s) [25]. The energies of these states relative to each other are not known. About $9{\cdot}10^4$ α particles from ^{193}Po were detected in total, $3{\cdot}10^4$ of them from the decay of the $3/2^-$ state. An RDT analysis was performed for both of the α-decay branches resulting in the prompt γ-ray spectra shown in Fig. 3a) and b). The energy resolution of the Si detector was not good enough to fully separate the two α peaks. Moreover, the relatively long half-lives resulted in increased amount of accidental correlations in the correlation analysis, thus increasing the number of background events in the γ-ray spectra. The energies and intensities of the γ-ray transitions assigned to ^{193}Po are listed in Table 3. The intensities are normalized to the most intense γ-ray transition in each spectrum.

A matrix of coincident γ-ray transitions tagged by the α decay from the $13/2^+$ state was constructed. The spectra with gates on the three strongest lines (251, 361 and 464 keV) clearly show that these transitions are in coincidence with each other. The level scheme built on top of the $13/2^+$ state of ^{193}Po is shown as an inset in Fig. 3b). The yrast band in the level scheme was built by using the intensity and coincidence information of the γ rays. The tentative spin assignments are based on the energy

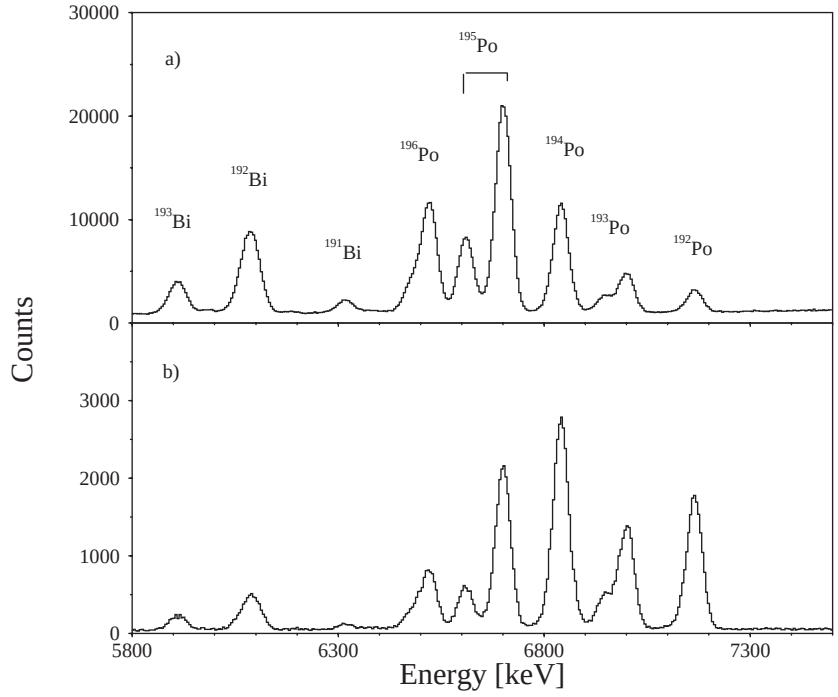

Fig. 1. a) Singles α spectrum from reaction ^{36}Ar(178MeV) + ^{160}Dy $\rightarrow$ ^{196}Po*. b) A recoil correlated α spectrum from the same reaction. The maximum correlation time was 170 ms

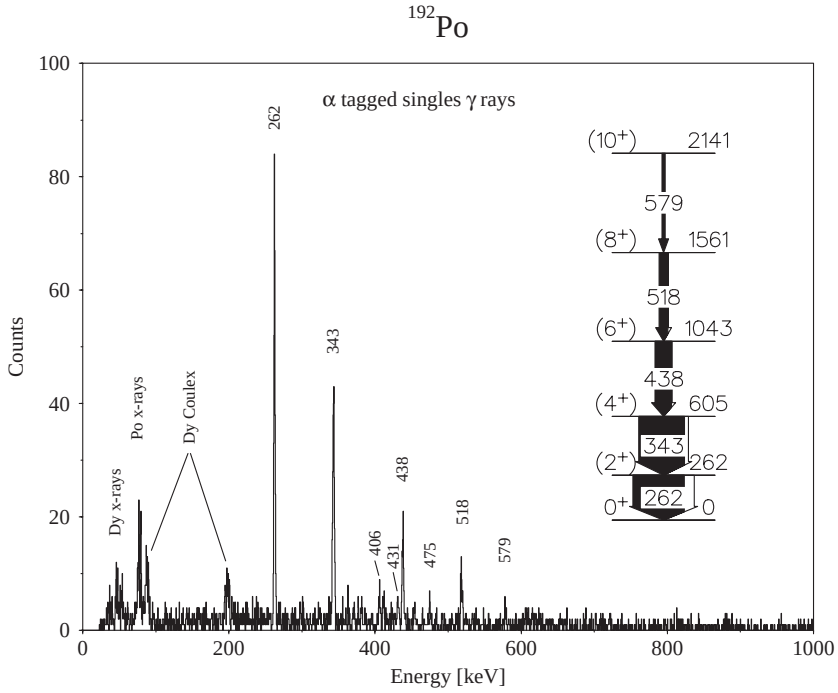

Fig. 2. Singles γ-ray spectrum tagged with ^{192}Po α decay. The deduced level scheme of ^{192}Po is as an inset

level systematics. The nonyrast part of the level scheme is based on the energy sums and intensities of the γ rays and is thus marked tentative.

A few γ-ray transitions were seen also on top of the $3/2^{-}$ state of ^{193}Po (Fig. 3a). Due to low statistics and lack of coincidences, construction of a level scheme was not possible.

The excited states in ^{193}Po have previously been studied by Fotiades et al. [17]. The observation of γ-ray transitions with energies of 251, 361, 368 and 486 keV was reported but the proposed level scheme differs from the one of this work. A transition of 234 keV, tentatively placed above the $3/2^{-}$ state, was not seen in our data.

3.3 ^{194}Po

The in-beam γ-ray data on ^{194}Po were collected in three runs dedicated to the production of this nucleus (experiments 2 - 4). In these runs a total of about 2 million

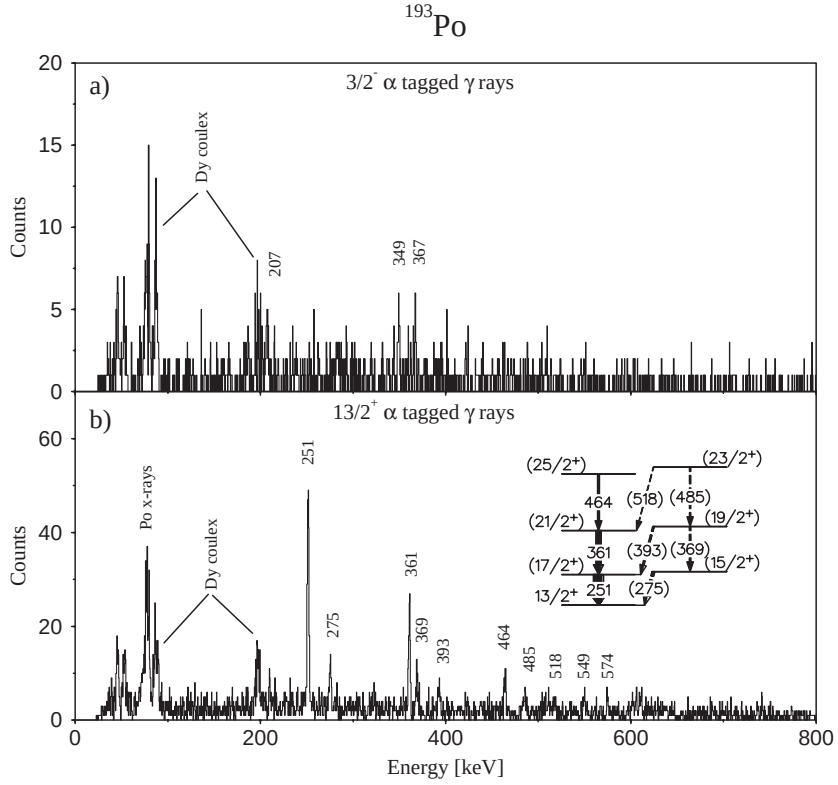

Fig. 3. a) Singles γ-ray spectrum tagged with the α decay of the $3/2^-$ state of ^{193}Po. b) Singles γ-ray spectrum tagged with the α decay of the $13/2^+$ state of ^{193}Po. The deduced level scheme above the $13/2^+$ state is as an inset

Table 3. γ-ray transitions and energy levels in ^{193}Po

E_γ (keV)	Intensity (%) [a]	E_i (keV)	I_i^π	I_f^π
γ-ray transitions above the $3/2^-$ state:				
206.7(5)	100(20)			
349.1(5)	100(40)			
367(1)	50(20)			
γ-ray transitions and energy levels above the $13/2^+$ state:				
251.4(5)	100(7)	251	$(17/2^+)$	$13/2^+$
274.9(5)	21(4)	275	$(15/2^+)$	$13/2^+$
360.9(5)	59(7)	612	$(21/2^+)$	$(17/2^+)$
369(1)	18(5)	644	$(19/2^+)$	$(15/2^+)$
393(1)	15(4)	644	$(19/2^+)$	$(17/2^+)$
463.7(5)	22(6)	1076	$(25/2^+)$	$(21/2^+)$
485(1)	15(5)	1129	$(23/2^+)$	$(19/2^+)$
518(1)		1129	$(23/2^+)$	$(21/2^+)$
549(1)	12(4)			
574(1)	7(3)			

[a] The intensities are normalised to the strongest transition in the both spectra

^{194}Po α decays were detected in about 12 days. The data from all of the experiments were put together and analysed using both the RDT and recoil-gating methods. The ^{194}Po half-life resulting from the analysis, 370(40) ms, is consistent with the literature value of 392(4) ms [25]. The total α tagged singles γ-ray spectrum for ^{194}Po is shown in Fig. 4a). Two $\gamma\gamma$ coincidence matrices were constructed, one from α tagged γ rays of ^{194}Po and the other from all the recoil gated γ rays. The level scheme of ^{194}Po was built by analysing these matrices with the RADWARE software package [26]. The α tagged γ rays of ^{194}Po from experiments 2 and 3 were sorted into two singles spectra, the other one consisting of the γ rays observed in the detectors at angle 143° and the other one of those observed in the detectors at angles 78° and 102°. The spin assignments were based on the angular distributions of the γ-ray transitions measured as the ratio I(143°)/I(∼90°) and on the level systematics. The I(143°)/I(∼90°) ratio for the well-known stretched E2 transitions in ^{196}Po seen in these experiments was 1.20(8). The level scheme consists of an yrast band extending to $I^\pi = (16^+)$ and a side band of low-lying 2_2^+, 4_2^+ and 6_2^+ states and odd-spin negative-parity states 7^- and 9^-. The sum of the spectra gated by the 545 keV and 602 keV peaks (Fig. 4b)) reveals the yrast transitions. The sum of the 434 keV and 454 keV gates is presented in Fig. 4c), showing other prompt transitions placed in the level scheme (except the 959 keV transition not seen in either of these gates). A 319 keV γ-ray transition was seen in coincidence with the 320 keV $2_1^+ \rightarrow 0_1^+$ transition but could not be placed into the level scheme, as well as the prompt γ-ray transitions of 359 keV and 803 keV.

The data on the isomeric state of ^{194}Po were obtained as a side product of the ^{193}Po α-decay experiment (experiment 6), where a total of about $1.7{\cdot}10^5$ ^{194}Po α decays were observed. The RDT method for the delayed γ rays was utilized, resulting in the spectrum shown in Fig. 4d). New γ rays having energies of 373, 459 and 918 keV, not observed in the prompt γ-ray spectrum, were tentatively assigned to form the de-excitation route from an isomeric

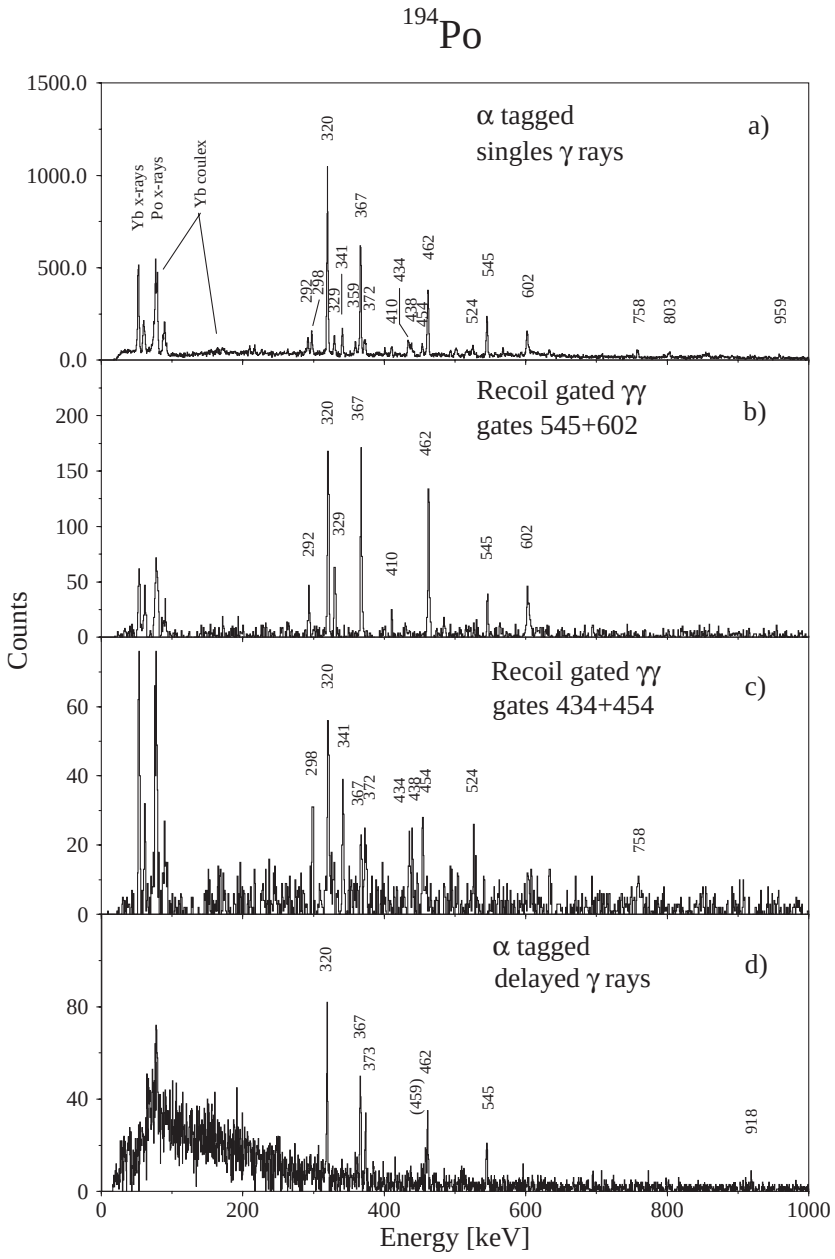

Fig. 4. a) Singles γ-ray spectrum tagged with the ^{194}Po α decay. b) Sum of the 545.2 keV and 601.8 keV gates set on the recoil gated $\gamma\gamma$ matrix. c) Sum of the 433.9 keV and 453.9 keV gates set on the recoil gated $\gamma\gamma$ matrix. d) Spectrum of delayed γ rays observed on the focal plane of RITU and tagged with the ^{194}Po α decay

state, suggested to have $I^{\pi} = 11^{-}$ similar to the isomer in ^{196}Po. A half-life of 15(2) μs was extracted for this state from the recoil-γ time distribution. No candidates for transitions to the lower 10^{+} and 9^{-} states were observed.

The level scheme of ^{194}Po based on the present experiments and containing both the prompt and the delayed γ-ray transitions is presented in Fig. 5. The γ-ray energies, intensities, angular distribution ratios, level energies, and the spin assignments are collected in Table 4. Excited states in ^{194}Po were first observed by Younes et al. [7]. Their level scheme extended up to a 2625 keV level assigned as an 11^{-} state and had tentative non-yrast 2_2^{+} and 4_2^{+} states at the energies 661 keV and 1211 keV. Our results extend and change the level scheme and add information on the intensities of the transitions. According to our new data the 341 keV transition is moved to feed the 1646 keV 6^{+} state and the non-yrast 2_2^{+} state has an energy of 758 keV. The spin and parity of the 2625 keV state is changed to 12^{+}, while the 11^{-} state is isomeric, having a tentative level energy of 2525 keV. It should be noted that our γ-ray energies are about 1 keV higher than those in [7].

3.4 ^{195}Po

The data on the excited states of ^{195}Po were collected in in-beam experiments 1 - 4. The nucleus ^{195}Po has two known α decaying states: the $3/2^{-}$ ground state (E_{α} = 6606(5) keV, $t_{1/2}$ = 4.64(9) s) and the isomeric $13/2^{+}$

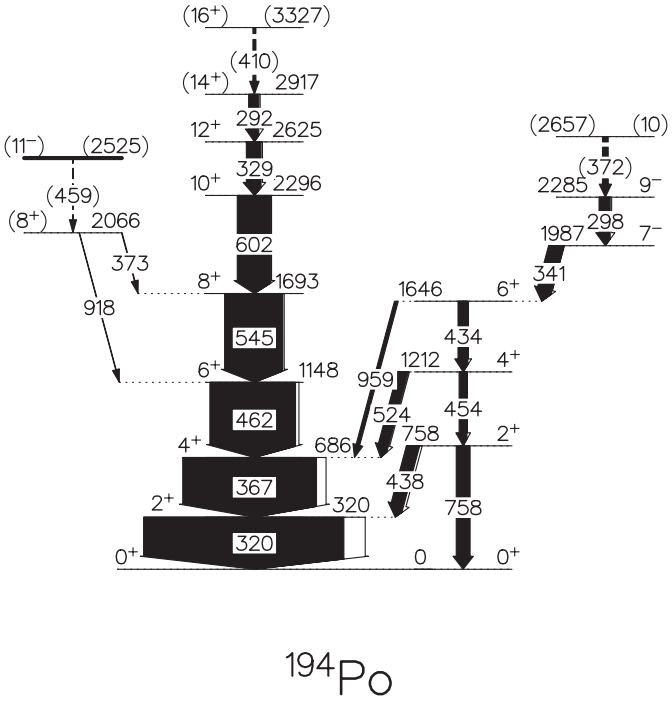

Fig. 5. Level scheme of ^{194}Po

Table 4. Properties of γ-ray transitions and energy levels in ^{194}Po

E_γ (keV)	Intensity (%)	E_i (keV)	I_i^π	I_f^π	I(143°)/ I(∼90°)
292.1(3)	5.1(7)	2917	(14^+)	12^+	
297.7(3)	5.6(9)	2285	9^-	7^-	1.5(4)
319.7(3)	100(8)	320	2^+	0^+	1.22(5)
329.2(3)	7.3(10)	2625	12^+	10^+	1.3(3)
340.8(3)	7.5(12)	1987	7^-	6^+	0.92(13)
359.2(5)	6(2)				0.7(2)
366.5(3)	66(7)	686	4^+	2^+	1.24(7)
371.9(5)	2.8(6)	(2657)	(10)	9^-	0.9(3)
373.1(5)		2066	(8^+)	8^+	
409.9(5)	1.4(5)	(3327)	(16^+)	(14^+)	
433.9(5)	4.9(12)	1646	6^+	4^+	1.2(6)
438.1(5)	6(2)	758	2^+	2^+	1.0(2)
453.9(5)	3.9(11)	1212	4^+	2^+	1.09(10)
458.6(5)		(2525)	(11^-)	(8^+)	
461.8(3)	43(5)	1148	6^+	4^+	1.30(10)
524.4(5)	5.1(12)	1212	4^+	4^+	0.8(3)
545.2(3)	29(3)	1693	8^+	6^+	1.18(11)
601.8(3)	17(2)	2296	10^+	8^+	1.3(3)
758.1(5)	7(5)	758	2^+	0^+	1.1(3)
802.7(5)	2(1)				0.9(4)
918.3(5)		2066	(8^+)	6^+	
958.7(5)	1.8(0.7)	1646	6^+	4^+	

state (E_α = 6699(5) keV, $t_{1/2}$ = 1.92(2) s) [25]. The isomeric state lies about 230 keV above the ground state [3]. A total of about $4{\cdot}10^5$ isomeric and $1{\cdot}10^5$ ground state α decays were observed in experiment 1. The number of α decays observed in experiments 2 - 4 was $1.6{\cdot}10^6$ and $0.4{\cdot}10^6$ for the isomeric and the ground state decay, respectively. An RDT analysis for both of the α decay branches was performed for the prompt γ-ray data from experiment 1. The resulting γ-ray spectra are shown in Fig. 6a) and b). The extracted transition energies, intensities, angular distribution ratios, level energies, and the spin assignments are listed in Table 5. As in the case of ^{193}Po the half-lives of the α decays were long considering the average counting rate in a detector pixel. This increased the amount of accidental correlations and thus the background in the γ-ray spectrum. Due to the high counting rate from the main reaction products the recoil-decay tagging analysis for ^{195}Po was not feasible for the data from experiments 2 - 4. However, the strongest transitions above the isomeric $13/2^+$ state were visible in the recoil gated $\gamma\gamma$ matrix. Using this matrix it was possible to observe that the transitions of 319, 388 and 494 keV were in coincidence with each other. In addition, a weak transition of 589 keV was observed in coincidence with the 388 and 494 keV transitions. The angular distributions of the three lowest transitions indicated E2 character for them. Using the γ-ray intensities and the previously mentioned facts as arguments a level scheme shown as an inset in Fig. 6b) was constructed. Tentatively, a side band similar to that in ^{193}Po could be formed from the 427 keV ($15/2^+ \rightarrow 13/2^+$), 404 keV ($19/2^+ \rightarrow 15/2^+$) and 510 keV ($19/2^+ \rightarrow 17/2^+$) transitions using energy sum and intensity arguments. A tentative level scheme on top of the isomeric $13/2^+$ state of ^{195}Po was previously published by Fotiades et al. [17]. Our level scheme confirms their scheme and adds the tentative side band above the $13/2^+$ state and one new level on top of the yrast cascade.

Table 5. Properties of γ-ray transitions and energy levels in ^{195}Po.

E_γ (keV)	Intensity (%)	E_i (keV)	I_i^π	I_f^π	I(143°)/ I(∼90°)
γ-ray transitions above the $3/2^-$ ground state:					
243.2(5)	60(20)				
319(1)	100(13)				
387(1)	61(14)				
406(1)	58(14)				
428(1)	90(30)				
γ-ray transitions and energy levels above the $13/2^+$ isomeric state:					
145(1)	3.7(8)				
187(1)	8.8(1.3)				
319.1(5)	100(4)	319	$17/2^+$	$13/2^+$	1.5(2)
323(1)	6.1(9)				
388.1(5)	55(4)	707	$21/2^+$	$17/2^+$	1.5(4)
404(1)	5.7(1.0)	831	$(19/2^+)$	$(15/2^+)$	
426.6(5)	17(2)	427	$(15/2^+)$	$13/2^+$	
494.3(5)	17(3)	1202	$25/2^+$	$21/2^+$	1.3(5)
510.0(5)	13(3)	831	$(19/2^+)$	$17/2^+$	
589(1)	6(2)	1791	$(29/2^+)$	$25/2^+$	

[a] The intensities are normalised to the 319 keV transition in the both spectra

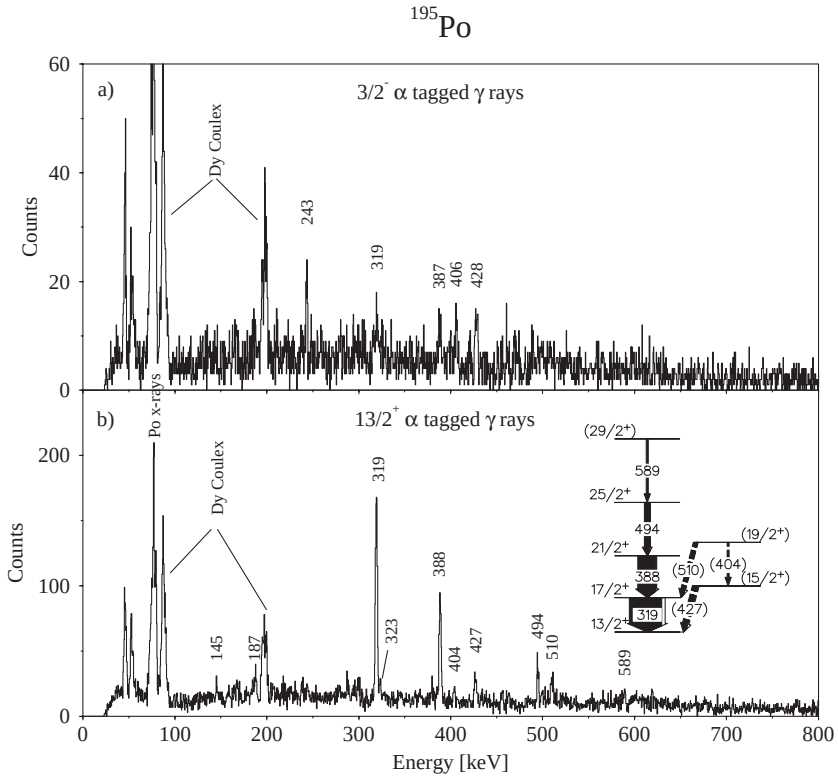

Fig. 6. a) Singles γ-ray spectrum tagged with the α decay of the $3/2^-$ ground state of ^{195}Po. b) Singles γ-ray spectrum tagged with the α decay of the $13/2^+$ isomeric state of ^{195}Po. The deduced level scheme above the $13/2^+$ state is as an inset

Several weak γ rays were observed in the spectrum tagged with the α decay of the $3/2^-$ ground-state of ^{195}Po (Fig. 6a). However, due to the low statistics it was not possible to order the transitions into a level scheme. The relatively long half-life of the state resulted in a high background. For this reason, the observed 319 keV and 387 keV peaks can be originated from the random coincidences with the much more abundantly produced $13/2^+$ state in ^{195}Po. Fotiades et al. [17] have reported on three γ transitions above the $3/2^-$ state, having energies of 230 keV, 427 keV and 470 keV. Only the 427 keV transition is clearly seen in our data. Also Taylor et al. [30] have listed γ transitions above the $3/2^-$ state of ^{195}Po. Their list seems to contain most of those transitions reported in both [17] and this work.

4 Interpretation

4.1 Systematics

A level systematics for even-mass $^{192-210}$Po isotopes including our new data for ^{192,194}Po are shown in Fig. 7. The positive parity low-lying yrast levels of the closed-shell nucleus ^{210}Po are formed by the proton $h^2_{9/2}$ multiplet. In the $^{200-208}$Po isotopes, neutron-hole orbitals are released for 2^+ and 4^+ broken pairs resulting in an increase of collectivity and a decrease of energy of the yrast 2^+_1 and 4^+_1 states. The level-energy behavior is rather smooth until at ^{198}Po, a drop of energies of the 2^+_1, 4^+_1 and 6^+_1 states is observed [4,5,13]. The energies of the yrast 8^+ states increase constantly until a sharp drop after ^{196}Po. With these states, in ^{192,194,196}Po also the 10^+ state drops down in energy. Signs of flattening in the level-energy systematics for the yrast levels $2^+ - 10^+$ is observed in ^{192}Po. Second excited 2^+_2 and 4^+_2 states have been identified for almost all currently studied Po isotopes.

The smoothly behaving negative-parity states 5^-, 7^- and 9^- were previously assigned as neutron states because of the similarity of their energies compared with similar levels in the Pb isotones [4]. This similarity seems to weaken in the lighter Po isotopes ^{194,196}Po. Isomeric 11^- states are observed in all the neutron-deficient Po nuclei with $110 \leq N \leq 126$.

4.2 Vibrational and rotational features

Based on in-beam γ-ray studies, Bernstein et al. have shown that ^{196,198}Po actually have features of quadrupole vibrational nuclei [13]. The same features are suggested to manifest themselves in ^{194}Po in [7]. This interpretation is based on the relatively constant energy spacings of the yrast levels as well as on the appearance of the 2^+_2 and 4^+_2 states in the vicinity of the 4^+_1 and 6^+_1 states forming a level structure reminiscent of that of a quadrupole-vibrational nucleus. The model is further argued by the E2 branching ratios determined for the 2^+_2 and 4^+_2 states. If these states were members of two- and three quadrupole-phonon multiplets, respectively, the $2^+_2 \rightarrow 0^+_1$ transition should be forbidden and the B(E2) ratio for the 4^+_2 state should be $B(E2;4^+_2 \rightarrow 2^+_2)/B(E2; 4^+_2 \rightarrow 4^+_1) = 1.1$.

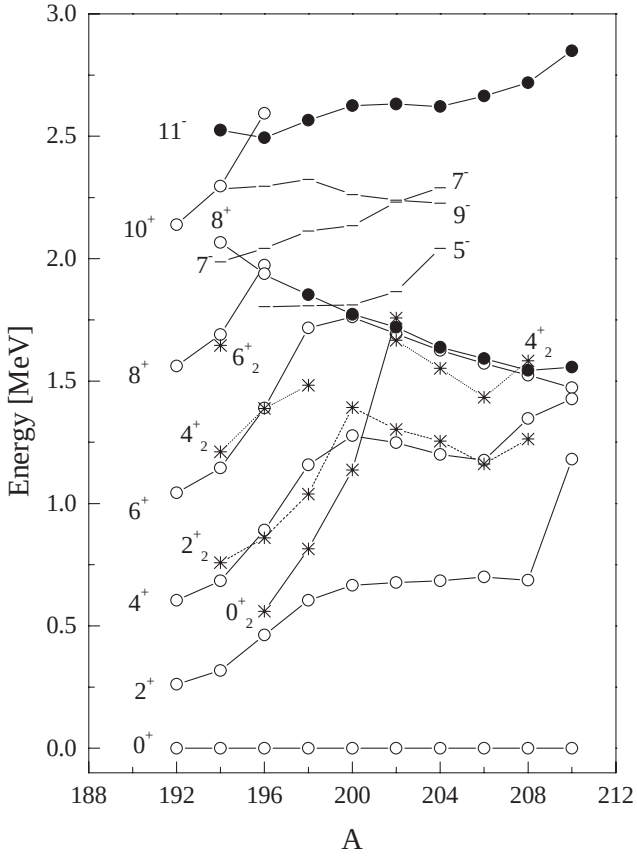

Fig. 7. Level systematics for even-mass $^{192-210}$Po isotopes. The yrast positive parity levels are marked with open circles, the non-yrast ones with asterisks and the negative parity levels are marked with bars. The isomeric states are assigned with filled circles

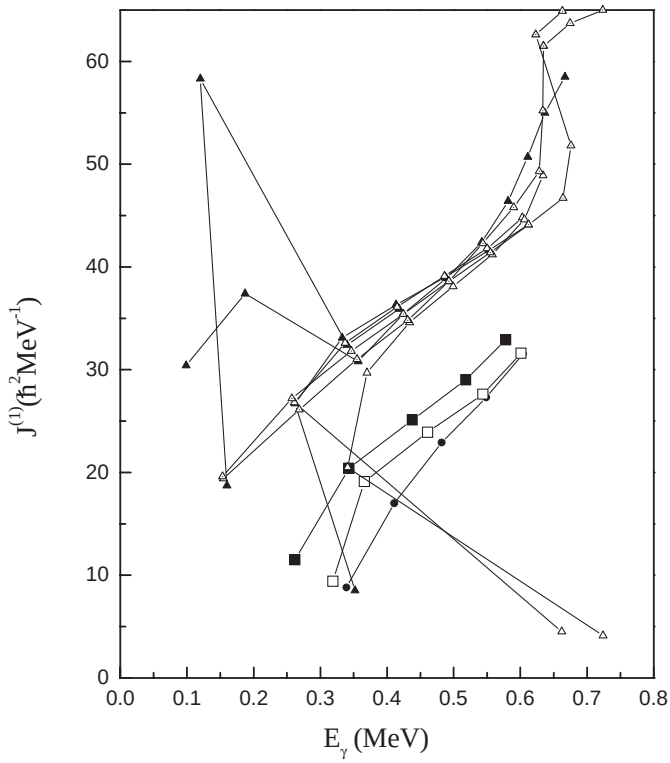

Fig. 8. Kinematic moment of inertia ($J^{(1)}$) as a function of the γ-ray transition energy for ^{192}Po (solid squares),^{194}Po (open squares) and ^{198}Rn (circles) compared to several even-mass ^{180,182}Pt (triangles with dots), $^{182-186}$Hg (solid triangles) and ^{186,188}Pb (open triangles) nuclei having a prolate deformed band

For ^{198}Po [13] and ^{196}Po [27] the $B(E2;2_2^+ \rightarrow 2_1^+)/B(E2;2_2^+ \rightarrow 0_1^+)$ ratios are 158(6) and 22(6), and the $B(E2;4_2^+ \rightarrow 2_2^+)/B(E2;4_2^+ \rightarrow 4_1^+)$ ratios 2.0(5) and 1.4(2), respectively, presuming that both branches are of pure E2 character. According to our results the corresponding values for ^{194}Po are 7(3) and 3.7(8). These ratios provide some evidence in support of the phonon picture in ^{194,196,198}Po although the values for ^{194}Po indicate that transition to some other kind of structure sets in. However, if the assumption of pure E2 character of the $\Delta I = 0$ transitions fails and they have some M1 component, the conclusions drawn from the B(E2) ratios are not valid any longer.

The simple quadrupole vibrator picture for the light Po isotopes is seriously disturbed by the behaviour of the first excited 0_2^+ state, which is observed to intrude down close to the 2_1^+ state in ^{196}Po [6]. Large anharmonicities would be needed to account for this state departing from the two-phonon triplet.

A recent study [9] of the de-excitation pattern of the non-yrast 2_2^+ and 0_2^+ states shows that a change in the nature of the low-lying positive parity non-yrast states takes place between the isotopes ^{200}Po and ^{202}Po. According to this study it is assumed that in the heavier isotopes (A$\geq$202) the positive parity states are members of quadrupole phonon multiplets whereas in the lighter nuclei (A$\leq$200) these states could belong to a deformed band intruding to low energies and mixing with the ground state band.

The yrast band in ^{192}Po and in ^{194}Po with regularly increasing level spacings up to the 10^+ state can be discussed within the framework of a soft rotor. In Fig. 8 the kinematic moments of inertia ($J^{(1)}$) for ^{192}Po and ^{194}Po have been plotted as a function of the γ-ray transition energy. The $J^{(1)}$ values extracted from the transitions above the 2^+ level follow a smoothly increasing trend. This behavior is typical for a soft rotor nucleus and can be described with a variable moment of inertia (VMI).

For comparison, the $J^{(1)}$ values for the intruder bands observed in ^{186,188}Pb and in even-A nuclei $^{182-186}$Hg (Z = 82 − 2) and ^{180,182}Pt (Z = 82 − 4) are shown in the same figure. Similarity between the intruder bands in the even-mass Pt, Hg and Pb isotopes close to the neutron midshell is well known [28]. These bands have been associated with a prolate minimum predicted in Nilsson-Strutinsky calculations [2,29]. Figure 8 shows how the moments of inertia for ^{192}Po and ^{194}Po behave qualitatively in the same way with the ones in the Pt, Hg and Pb isotopes except that

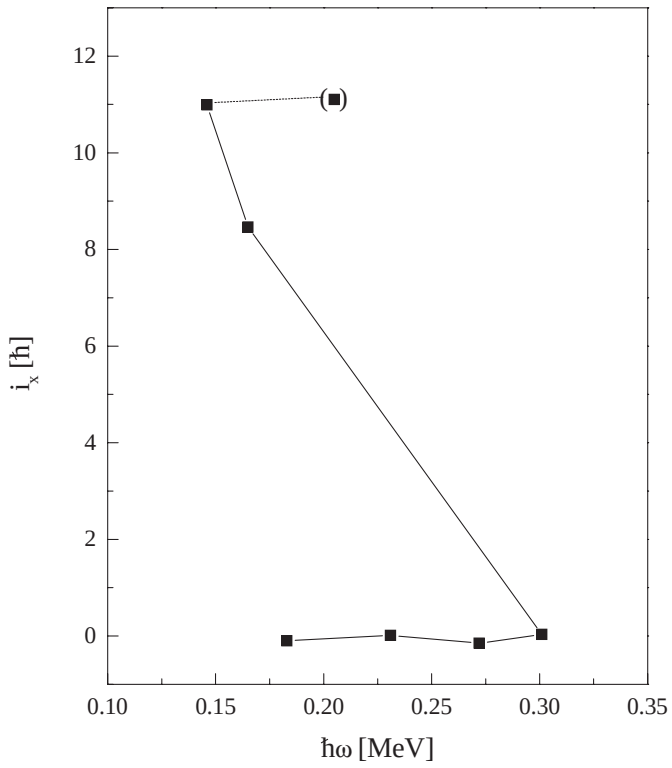

Fig. 9. Aligned angular momentum i_x for the yrast band in ^{194}Po. A reference with Harris parameters $J_0 = 12.8\ \hbar^2/MeV$ and $J_1 = 205.8\ \hbar^4/MeV^3$ has been subtracted

the $J^{(1)}$ values are systematically about 10 $\hbar^2$/MeV lower. The moments of inertia for the yrast band of ^{198}Rn extracted from a recent RDT study [30], are also shown in Fig. 8 revealing that intruder structures similar to those in ^{192}Po and ^{194}Po also become yrast in very neutron deficient even-mass Rn isotopes. These structures can represent the oblate minimum which according to calculations [2] should reach the ground state in ^{192}Po.

The smooth behavior of the transition energies of the yrast band in ^{194}Po ends when the 10^+ state is passed. Considering this change from the view of the rotational scheme the single-particle alignments (i_x) in a nucleus may be observed when the angular momentum of the collective rotation is subtracted from the total angular momentum. In Fig. 9 this alignment i_x in ^{194}Po is plotted as a function of the rotational frequency $\hbar\omega$. The ground state rotational band with $i_x \approx 0$ persists until at $\hbar\omega \approx 0.3$ MeV a sharp alignment takes place. The gain obtained in the alignment is about 11 $\hbar$ which is consistent with that for the alignment of two $i_{13/2}$ neutrons.

The level structure of ^{194,196,198}Po could also be described by means of the rotation-vibration interaction in non-axial even-mass nuclei [31]. Within this model, the observed $E_{2_2^+}/E_{2_1^+}$ ratios in ^{196,198}Po are best reproduced with maximum triaxiality ($\gamma = 30°$) and softness ($\mu = 1$) [32,33]. For ^{194}Po the respective values would be $\gamma \approx 25°$ and $\mu \approx 0.6$. This could be interpreted as a beginning of development towards an axial shape. The problem in the feasibility of this model is the non-observation of the low-lying 3^+ state, as was pointed out already in [5]. Also, the application of this model to ^{192}Po has to wait until the possible second excited levels are known.

4.3 Intruder structures

The intruding oblate structures in light Po isotopes are associated with two-proton excitations across the Z = 82 gap (*4p-2h* states) [6]. Based on the simple intruder mechanism an intruder analog scheme was introduced by Heyde et al. [34]. They suggest that the deformed intruder states can be classified according to their intruder spin which is defined by $I^{(i)} = N_{val}/2$ and $I_z^{(i)} = (N_{val,p} - N_{val,h})/2$, where N_{val} is the number of the valence particle- and hole pairs and $N_{val,p}$ ($N_{val,h}$) is the number of the valence particle (hole) pairs. In this scheme the bosons formed by the particle and hole pairs are treated on the same footing giving rise to intruder spin multiplets with nuclei having similar types of energy level structure. According to this model the rotational bands in Po and Hg isotones, based on the *4p-2h* and *2p-4h* intruder states, respectively, and the ground state band in Os (*6h*), all belonging to the $I^{(i)} = 3/2$ multiplet, should be similar. De Coster et al. have compared the energy-level structure of light Po and Os isotones and found that once the local mixing of the intruder and regular states is excluded, the $I^{(i)} = 3/2$ multiplet is recovered approximately [35]. However, our comparison between the $J^{(1)}$ values of these bands showed only weak similarities that could also be coincidental. Also the data in Fig. 8, showing the supposed Po intruder bands compared to the observed prolate bands in Hg nuclei disagree with this scheme. The contradiction with the Hg isotones can be avoided by suggesting that the prolate states in Hg nuclei, similarly to the respective Pb nuclei, belong into even higher excited groups formed by $I^{(i)} = 5/2$ (*4p-6h* state) multiplet ($I^{(i)} = 2$ or 3 (*4p-4h* or *6p-6h* states) multiplets in Pb) [29].

This leaves a question about the existence of $I^{(i)} = 3/2$ bands in Hg and $I^{(i)} = 1$ bands in Pb nuclei, especially because the intruder 0^+ states showing *2p-2h* properties are observed in the $A \geq 188$ Pb isotopes in α-decay studies [36]. On the other hand, while the prolate bands in the intruder spin multiplets of $I^{(i)} = 2$ and $I^{(i)} = 5/2$ are very similar, it can be seen (Fig. 8) that at high spin the $J^{(1)}$ values of ^{198}Rn, the lightest Z = 86 isotope with known excited states [30], show the same pattern as the supposed *4p-2h* states ($I^{(i)} = 3/2$) of ^{192}Po and ^{194}Po.

Another analogy scheme for the Pb region is presented by Barrett et al. [37] who suggest that the shape-coexisting intruder states are members of F-spin multiplets formed by nuclei differing by an α particle. In the F-spin scheme [38] the valence proton and neutron pairs form bosons having a total F-spin value of $F = (N_\nu + N_\pi)/2$, where N_ν and N_π are the number of neutron and proton bosons, respectively. The multiplet is formed by the nuclei having the same F spin but different projections $F_0 = (N_\nu - N_\pi)/2$. This analogy fits well for the

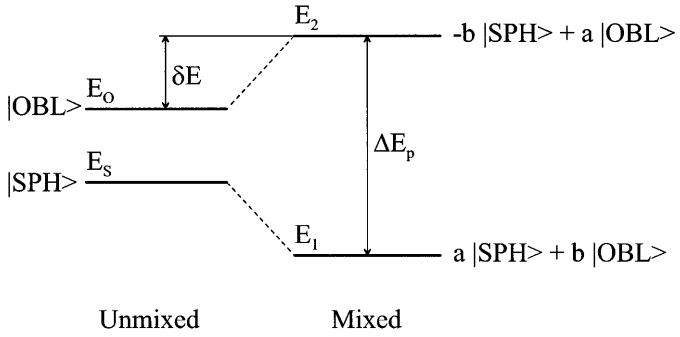

Fig. 10. Schematic drawing of two-level mixing between the spherical (SPH) and oblate (OBL) deformed states

similarity between ^{194}Po and ^{198}Rn (Fig. 8) but is hard to confirm in ^{190}Pb where no oblate band has been identified.

In the simple picture of the proton intruder states, it rather looks as if the two proton holes in the Z = 82 shell are associated with the oblate minimum (the ground state of even-A Hg, the *2p-2h* 0_2^+ states in Pb with A $\geq$ 188, the *4p-2h* state(s) in Po and the possible *6p-2h* band in ^{198}Rn). In a similar way the prolate shape could be connected to four holes in the Z = 82 shell (prolate bands in Pt, Hg and Pb). The predicted prolate structure in the Po nuclei near the neutron midshell [2] could then originate from the *4p-4h* proton excitations across the shell gap (*6p-4h* state). Unfortunately, due to very low production cross-sections, it is difficult to probe structures of Z > 82 nuclei close the neutron midshell.

4.4 Coexisting structures

As seen in Fig. 8, for the ^{192}Po and ^{194}Po isotopes the $J^{(1)}$ values derived from the 0_1^+ - 2_1^+ energy difference are clearly smaller than the values extrapolated from the higher spin states. These irregularities can be due to crossing and mixing of two different coexisting structures. We have tested this interpretation by a simple two-level mixing calculation, similar to that performed by Oros et al. [16]. In these calculations the experimentally observed states are formed when close-lying pure spherical and deformed (oblate in this case) states with same spin and parity interact (see Fig. 10). As a result of the interaction the states get mixed and repel each other. The mixing amplitude b can be obtained from the formula [16]

$$\delta E = b^2 \Delta E_p, \qquad (1)$$

where δE is the energy difference between the unperturbed and perturbed (experimental) states and ΔE_p the difference between the two perturbed states.

The low-spin level energies of the unperturbed oblate band in ^{192}Po and ^{194}Po are extrapolated from the experimental energies of the 4^+, 6^+, 8^+ and 10^+ levels, which are assumed to be unmixed members of the oblate band. Because the first excited 0^+ states (0_2^+) are not experimentally observed in ^{192}Po and ^{194}Po the values for the perturbed energies of these states were taken from the work of Oros et al. [16]. These values are obtained from the potential energy surface (PES) calculations which in heavier Po isotopes give 0_2^+ energies very close to the experimentally observed ones.

Unperturbed level energies obtained from the mixing calculation are shown in Fig. 11. The energies are normalised to the experimental 0^+ ground state (0_1^+). It is interesting to see that the deformed bandhead 0^+ state, which in ^{194}Po is still slightly above the spherical one, has become the ground state structure in ^{192}Po. In the experimentally observed levels the mixture of the deformed state in the 0_1^+ ground state increases from 45% in ^{194}Po to 73% in ^{192}Po. This change was also proposed by Bijnens et al., who got a corresponding value of 58% for the ground state of ^{192}Po using the energy systematics [6]. Similarly, Allatt [39] et al. and Andreyev et al. [40], on the basis of the α-decay studies, extracted the values of $\sim$ 63% and > 65%, respectively, for the intruder mixture in the ground state of ^{192}Po. The observed 2_1^+ state of ^{194}Po is 99% of deformed structure. This value is calculated using our new 2_2^+ level energy. A similar value can be expected also for the 2_1^+ state in ^{192}Po by comparing the experimental 2_1^+ energy with the one extrapolated from the energies of the higher spin states.

It is interesting to note that the unperturbed spherical $0^+ - 2^+$ energy difference is very similar to the experimentally observed $0_1^+ - 2_1^+$ difference in the heavier polonium nuclei with A = 200 - 208. This is in accordance with the scheme of having the level structure of ^{194}Po as the spherical normal states crossed by the deformed intruder states. Using an empirical fit to the available data, the absolute value of deformation parameters β_2 can be estimated from the $2^+ \rightarrow 0^+$ transition energy [41]. In this way $|\beta_2|$ values for the unperturbed intruder bands in ^{194}Po and ^{192}Po can be estimated to be about 0.17 and 0.18, respectively. They are not far from the theoretically predicted [2,16] oblate deformation parameters $|\beta_2| \approx 0.2$.

4.5 E0 transitions

Considerable E0 components in the $4_2^+ \rightarrow 4_1^+$ and $2_2^+ \rightarrow 2_1^+$ transitions of ^{198}Po have been reported by Alber et al. [5] on the basis of missing γ-ray intensities. This observation was used as an evidence to support the view of mixed coexisting structures of different shapes. However, in the more recent measurements Bernstein et al. [13] could not find any evidence for strong E0 components in the same transitions of ^{198}Po as well as of ^{196}Po. This result was used as an argument against the deformed intruder picture and to support the vibrational view. From our $\gamma\gamma$ coincidence data we have extracted, for the corresponding transitions in ^{194}Po, percentages of 8$\pm$33% and 38$\pm$20%, respectively, for the missing γ-ray intensities. In the following we consider more closely the E0 transitions in ^{194}Po, ^{196}Po and ^{198}Po and their appearance as measurable E0 components.

In the simple coexistence model electric monopole transitions are allowed between spherical and deformed states of same spin and parity only if these states are

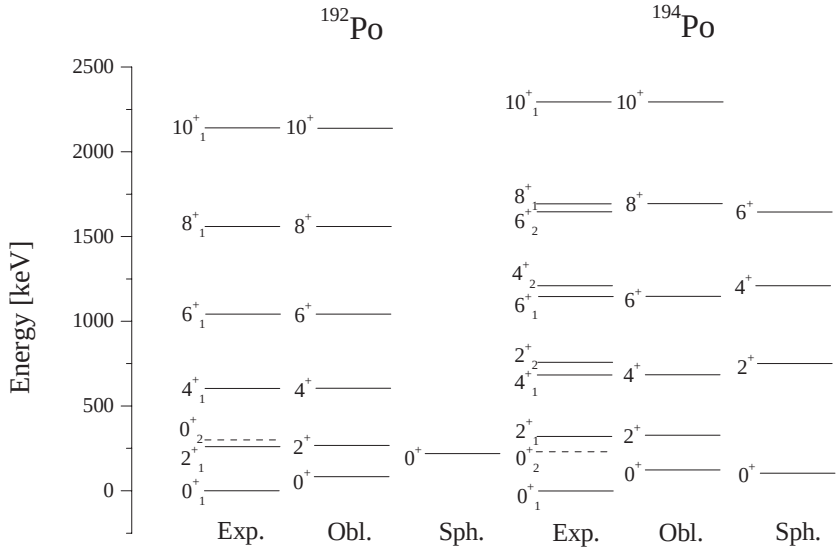

Fig. 11. Experimental and unperturbed spherical and oblate deformed level energies in ^{192}Po and ^{194}Po. The 0_2^+ level energies are taken from the calculations in [16]. The energies are normalized to the experimental 0_1^+ states

mixed [42]. The monopole strength parameter ρ can be obtained from the formula [42,43]

$$\rho \approx abk\beta_2^2, \tag{2}$$

where a and b are the mixing amplitudes, β_2 is the deformation parameter and

$$k = (3/4\pi)ZeR^2[1 + (4\pi/3)(a_0/R)^2], \tag{3}$$

where a_0 is the diffuseness parameter of the nuclear surface and R is the nuclear radius [44]. The low-energy E0 transitions proceed via internal conversion and the transition probability can be written as

$$\lambda(E0) = \rho^2 \sum_i \Omega_i, \tag{4}$$

where Ω_i is the energy-dependent electronic factor for $i = K, L, ...$ conversion [45]. The ρ^2 values for the $2_2^+ \rightarrow 2_1^+$ and $4_2^+ \rightarrow 4_1^+$ transitions in ^{194}Po, ^{196}Po and ^{198}Po were calculated by using the mixing amplitudes obtained from [16] and the present work. The deformation parameter β_2 = -0.2 predicted for the oblate structure both in [2] and [16] was used. The resulting ρ^2 values shown in Table 6 demonstrate how the E0 rates can vary in the adjacent even-mass Po isotopes because of different mixing between the states involved. It should also be noted that the E0 transition rate is related to fourth power of the deformation parameter β_2. Consequently, the ρ^2 values given in Table 6 would be reduced by factor of two if the deformation parameter β_2 would turn out to be -0.17 instead of -0.2.

The actual contribution of the E0 transitions in the observed intensities depends on the speed of the competing E2 or M1 γ-ray transitions. By using the ρ^2 values of Table 6 and by assuming pure E2 character for the competing γ-ray transitions, estimates for the E0 contributions in the $2_2^+ \rightarrow 2_1^+$ and $4_2^+ \rightarrow 4_1^+$ transitions in ^{194}Po, ^{196}Po and ^{198}Po were derived. These estimates in the cases of the competing E2 rates being of 1, 10 and 100 Weisskopf units, are shown in Table 7. In this table corresponding experimental E0 contributions obtained in the present work (^{194}Po) and derived from the data given in [5] (^{198}Po) and in [13] (^{196}Po, ^{198}Po) are also presented. This table together with the facts related to Table 6 demonstrates how difficult it is, without information about the competing γ-ray transition rates, to draw any decisive conclusion about deformation for the states involved. It is interesting to note that, taking the error bars into account, the E0 contributions in the transitions of ^{198}Po taken from the data of [5] and [13] and shown in Table 7 are consistent. Still the conclusions drawn from these results were contradictory.

Table 6. Calculated ρ^2 values for the $2_2^+ \rightarrow 2_1^+$ and $4_2^+ \rightarrow 4_1^+$ monopole transitions in ^{194,196,198}Po

Nucleus	$\rho^2(2_2^+ \rightarrow 2_1^+)$ (10^{-3})	$\rho^2(4_2^+ \rightarrow 4_1^+)$ (10^{-3})
^{194}Po	10	0
^{196}Po	152	178
^{198}Po	28	173

4.6 Isomeric states

In neutron deficient even-mass Po isotopes isomeric states with $I^\pi = 8^+$, 11^- and 12^+ have been found [4,5,46]. In the isotopes from ^{210}Po down to ^{198}Po the 8^+ isomer can be associated with the $\pi h_{9/2}^2$ multiplet. Due to the sudden drop of the energy of the yrast 6^+ state this 8^+ state is no longer isomeric in ^{196}Po.

Isomeric 12^+ states of the $\nu i_{13/2}^2$ configuration are observed in the even-A polonium isotopes from ^{202}Po to ^{198}Po [4].

The third observed isomer, with $I^\pi = 11^-$, has been found in all of the neutron deficient even-mass Po isotopes down to ^{196}Po. The g-factors measured for these states [4] reveal their dominant configuration of $\pi h_{9/2} i_{13/2}$. The

Table 7. Estimated percentages of E0 transitions of all the transitions between equal spin states of ^{194,196,198}Po. The values are calculated for three different E2 strengths and compared with measured missing γ-ray intensity values ([5,13] and this work)

Transitions	B(E2)=1W.u.	B(E2)=10W.u.	B(E2)=100W.u.	[5]	[13]	This work
^{194}Po($2_2^+ \rightarrow 2_1^+$)	75%	23%	3%			38±20%
^{194}Po($4_2^+ \rightarrow 4_1^+$)	0%	0%	0%			8±33%
^{196}Po($2_2^+ \rightarrow 2_1^+$)	99%	88%	42%		≤21%	
^{196}Po($4_2^+ \rightarrow 4_1^+$)	97%	75%	23%		≤55%	
^{198}Po($2_2^+ \rightarrow 2_1^+$)	89%	45%	8%	34±10%	11±42%	
^{198}Po($4_2^+ \rightarrow 4_1^+$)	99%	95%	64%	≥67%	49±29%	

B(E3) values for the $11^- \rightarrow 8^+$ transitions strongly increase with decreasing neutron number, reaching a value of 27(5) W.u. in ^{196}Po [5]. This is taken as an indication of the onset of collective E3 admixture in this transition and a possible appearance of a low-lying collective 3^- state. From our tentative result for the corresponding transition in ^{194}Po a B(E3) value of 8.4(12) W.u. was extracted. This value indicates weakening of the octupole collectivity compared to the heavier Po isotopes. However, the identification of the 459 keV $11^- \rightarrow 8^+$ transition was not firm. If the transition energy is calculated from the B(E3) value of ^{196}Po and the observed half-life in ^{194}Po, a value of about 387 keV is obtained. On the other hand, the existence of a 12^+ isomer possibly feeding the 11^- isomer cannot be ruled out. This feeding could increase the half-life measured for the 11^- state and thus result seemingly in the B(E3) value being smaller than expected.

The decay of the isomeric 11^- state in Po isotopes with N = 114 - 118, 124, 126 proceeds via the $\pi h_{9/2}^2$ 8^+ state. It could be expected that also in the more collective ^{194,196}Po nuclei the 11^- state would still de-excite to the 8^+ state with a dominant $\pi h_{9/2}^2$ configuration. Therefore the yrast 1939 keV 8^+ state in ^{196}Po and the non-yrast 2066 keV (8^+) state in ^{194}Po can be associated with the $\pi h_{9/2}^2$ configuration.

4.7 Odd-mass nuclei

In Fig. 12 energies of yrast levels of the even-mass neutron-deficient Po nuclei are shown together with the level structure built on top of the isomeric $13/2^+$ state in the odd mass Po nuclei. Especially in the lightest isotopes the level patterns of the odd mass nuclei are close to the ones of the adjacent even mass isotopes. This indicates a weak coupling of the $i_{13/2}$ neutron to the even-mass core which could be regarded as a coupling of the odd $i_{13/2}$ neutron to a vibrating spherical core [17] or, in accordance with the rotational and intruder picture, as a decoupling of an $i_{13/2}$ neutron hole (low Ω) from the oblate core. In ^{193}Po and ^{195}Po we have found candidates for the $15/2^+$, $19/2^+$ and $23/2^+$ states of the unfavoured $i_{13/2}$ band. In ^{193}Po the unfavoured states come down closer to the favoured ones indicating a change towards strong-coupling scheme when the number of neutron holes increases. This behavior is characteristic to oblate deformation since the Ω increases and thus the Coriolis force decreases when depleting the

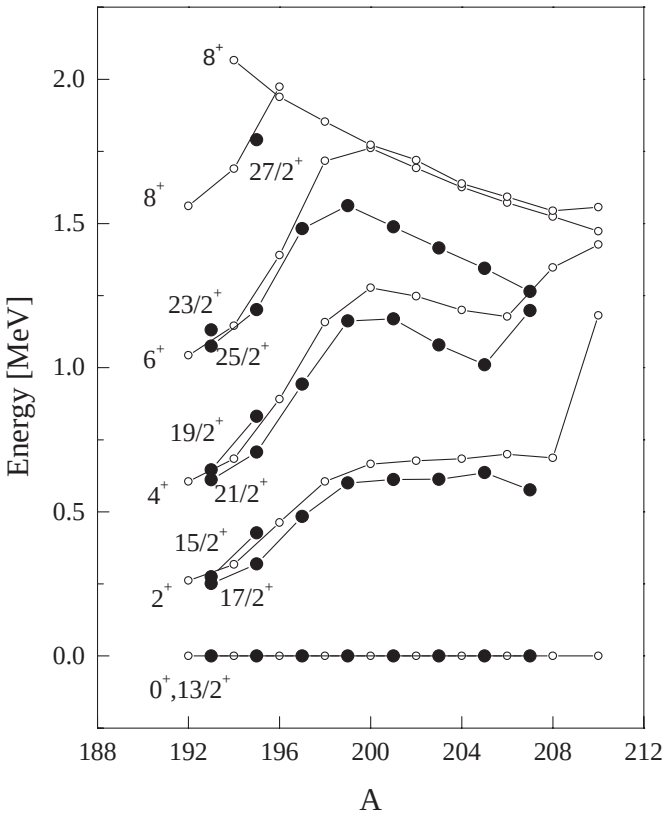

Fig. 12. Energies of the yrast levels of the even-mass $^{192-210}$Po nuclei (open circles) together with the levels built on top of the $13/2^+$ states in the odd-mass $^{193-207}$Po nuclei (filled circles)

$i_{13/2}$ shell. Thus, the observation of a low-lying unfavoured spin band in ^{195,193}Po is in agreement with the picture of the onset of oblate deformation at low spins in light Po nuclei with N ≈ 108.

5 Summary

Comprehensive γ-ray spectroscopic studies of very neutron-deficient $^{192-195}$Po nuclei have been carried out by employing the recoil-decay tagging (RDT) and recoil gating methods for both prompt and delayed γ rays. The yrast line up to the (10^+) state in the ^{192}Po isotope, produced with a cross section of only about 10 μb, was identified for the first time. The $\gamma\gamma$-coincidence and angular-

distribution information for ^{194}Po enabled the yrast states to be extended up to (16^+) and the identification of the second excited 2^+, 4^+, 6^+, (8^+) and (10) states as well as the negative parity 7^-, 9^- and isomeric (11^-) states. In the odd-mass isotopes ^{193}Po and ^{195}Po, yrast and nonyrast states on top of the $13/2^+$ state have been identified.

Our new data are in accordance with the picture of the coexisting normal spherical and intruding oblate states crossing each other when going to the Po isotopes with N < 114. The new data for ^{192}Po reveals signs of flattening of the level-energy systematics. This, together with the simple mixing calculations show that the intruder structures have reached the ground state at N = 108 as predicted earlier in the Nilsson-Strutinsky type of calculations [2]. Comparison of the yrast-level energies of the light odd- and even-mass Po isotopes show that the $i_{13/2}$ neutron is weakly coupled to the even-mass core. The observed behavior of the unfavoured states can be explained by this coupling if the core has an oblate shape.

Many of the observed properties of light Po isotopes can also be described within the simple quadrupole vibrational model. The studies of the midshell Cd [47] and Te [48] nuclei have lead to a paradoxical conclusion: in these nuclei the 0^+ and 2^+ proton intruder states clearly take part in generating low-lying quadrupole 2- and 3-phonon multiplets. Thus, there is not necessarily any contradiction between the simple vibrational and the coexistence pictures: the microscopic structure of a quadrupole phonon could include a proton intruder component.

We are grateful for the staff at JYFL for providing excellent beams and technical support. The authors gratefully acknowledge Andrei Andreyev, Karen Van De Vel, Mark Huyse and Piet Van Duppen for allowing the use of their experimental data in this work. This work was supported by the Academy of Finland and the Access to Large Scale Facility program under the Training and Mobility of Researchers (TMR) program of the European Union (EU). R.G.A., P.A.B., P.T.G. and R.D.P. acknowledge financial support from the EPSRC. P.J. acknowledges EU for a TMR research grant.

References

1. J.L. Wood *et al.*, Phys. Rep. **215**, 101 (1992)
2. F.R. May *et al.*, Phys. Lett. **B 68**, 113 (1977)
3. R.B. Firestone *et al.*, *Table of Isotopes*, 8th ed. Vol. II, (John Wiley & sons inc., New York 1996)
4. A. Maj *et al.*, Nucl. Phys. **A 509**, 413 (1990)
5. D. Alber *et al.*, Z. Phys. **A 339**, 225 (1991)
6. N. Bijnens *et al.*, Phys. Rev. Lett. **75**, 4571 (1995)
7. W. Younes *et al.*, Phys. Rev. **C 52**, R1723 (1995)
8. K. Helariutta *et al.*, Phys. Rev. **C 54**, R2799 (1996)
9. N. Bijnens *et al.*, Phys. Rev. **C 58**, 754 (1998)
10. J. Wauters *et al.*, Z. Phys. **A 344**, 29 (1992)
11. J. Wauters *et al.*, Phys. Rev. Lett. **72**, 1329 (1994)
12. N. Bijnens *et al.*, Z. Phys. **A 356**, 3 (1996)
13. L.A. Bernstein *et al.*, Phys. Rev. **C 52**, 621 (1995)
14. N. Fotiades *et al.*, Phys. Rev. **C 55**, 1724 (1997)
15. W. Younes *et al.*, Phys. Rev. **C 55**, 1218 (1997)
16. A. Oros *et al.*, Nucl. Phys. **A 645**, 107 (1999)
17. N. Fotiades *et al.*, Phys. Rev. **C 56**, 723 (1997)
18. R.S. Simon *et al.*, Z. Phys. **A 325**, 197 (1986)
19. E.S. Paul *et al.*, Phys. Rev. **C 51**, 78 (1995)
20. A.N. Andreyev *et al.*, Phys. Rev. Lett. **82**, 1819 (1999)
21. A.N. Andreyev *et al.*, to be published
22. M. Leino *et al.*, Nucl. Instr. Meth. **B 99**, 653 (1995)
23. P.J. Nolan *et al.*, Nucl. Instr. Meth. **A 236**, 95 (1985)
24. C.W. Beausang *et al.*, Nucl. Instr. Meth. **A 313**, 37 (1992)
25. J. Wauters *et al.*, Phys. Rev. **C 47**, 1447 (1993)
26. D.C. Radford, Nucl. Instr. Meth. **A 361**, 297 (1995)
27. J.A. Cizewski *et al.*, in *Proceedings of conference ENAM98: Exotic Nuclei and Atomic Masses, Bellaire, Michigan, 1998*, edited by B.M. Sherrill, D.J. Morrissey, C.N. Davids (AIP Conference proceedings 455, Woodbury, New York, 1998), p. 486.
28. G.D. Dracoulis, Phys. Rev. **C 49**, 3324 (1994)
29. W. Nazarewicz, Phys. Lett. **B 305**, 195 (1993)
30. R. Taylor *et al.*, Phys. Rev. **C 59**, 673 (1999)
31. A.S. Davydov *et al.*, Nucl. Phys **20**, 499 (1960)
32. R.F. Casten, *Nuclear Structure from a Simple Perspective*, (Oxford University Press, New York 1990)
33. A.S. Davydov *et al.*, Sov. J. Nucl. Phys. **3**, 740 (1966)
34. K. Heyde *et al.*, Phys. Rev. **C 46**, 541 (1992)
35. C. De Coster *et al.*, Nucl. Phys. **A 651**, 31 (1999)
36. P. Van Duppen *et al.*, Phys. Rev. Lett. **52**, 1974 (1984)
37. B.R. Barrett *et al.*, Phys. Rev. **C 43**, R926 (1991)
38. A. Arima *et al.*, Phys. Lett. **B 66**, 205 (1977)
39. R. Allatt *et al.*, Phys. Lett. **B 437**, 29 (1998)
40. A.N. Andreyev *et al.*, J. Phys. **G 25**, 835 (1999)
41. L. Grodzins, Phys. Lett. **2**, 88 (1962)
42. J. Kantele *et al.*, Z. Phys. **A 289**, 157 (1979)
43. Jan Blomqvist, private communication 1978
44. A. Bohr, B.R. Mottelson, *Nuclear Structure*, Vol. II, (W.A. Benjamin Inc., Reading 1975)
45. D.A. Bell *et al.*, Can. J. Phys. **48**, 2542 (1970)
46. A. Maj *et al.*, Z. Phys. **A 324**, 123 (1986)
47. J. Kumpulainen *et al.*, Z. Phys **A 335**, 109 (1990)
48. S. Juutinen *et al.*, to be published